



Transcriptome analysis of a compatible response by *Glycine max* to *Phakopsora pachyrhizi* infection

Arianne Tremblay^{a,*}, Parsa Hosseini^b, Nadim W. Alkharouf^b, Shuxian Li^c, Benjamin F. Matthews^a

^a USDA-Agricultural Research Service (ARS), Plant Sciences Institute, Soybean Genomics and Improvement Laboratory, 10300 Baltimore Avenue, Beltsville, MD 20705, USA

^b Towson University, 8000 York Road, Towson, MD 21252, USA

^c USDA-ARS, Crop Genetics Research Unit, Stoneville, MS 38776, USA

ARTICLE INFO

Article history:

Received 5 March 2010

Received in revised form 27 April 2010

Accepted 27 April 2010

Available online 10 May 2010

Keywords:

Microarray

Soybean

Soybean rust

Fungus

Plant

Metabolic pathway

ABSTRACT

Soybean is one of the top five agricultural products in the United States. Soybean rust is caused by the obligate fungus *Phakopsora pachyrhizi* Sydow, an exotic pathogen in the U.S. Extensive screening of soybean germplasm has not identified soybean with resistance to all of the different isolates of soybean rust. A biotechnological approach may help to understand the plant host response at the molecular level and subsequently broaden resistance of soybean to this fungus. Using laser capture microdissection, we isolated susceptible soybean palisade and mesophyll cells showing signs of infection, extracted the RNA and performed transcriptome profiling. A total of 2982 genes were found to be differentially expressed, of which 685 were up-regulated, and 2297 were down-regulated. Eighty-eight percent of our regulated genes are unique to our time-point and our palisade cells. Gene expression data was overlaid on Kyoto Encyclopedia of Genes and Genomes biochemical pathways. In general, up-regulated genes were associated with basic defense while down-regulated genes were associated with many metabolic pathways. These results demonstrate that soybean rust strongly affects plant metabolism at the latest stage of infection and that the plant futilely fights even at the end of the infection process to establish a resistance response.

Published by Elsevier Ltd.

1. Introduction

The infection of soybean by the obligate biotrophic fungus *Phakopsora pachyrhizi* Sydow, which causes rust on soybean as well as on a wide range of hosts, is still new in the United States. It is expected to be responsible for large yield losses throughout the country. A recent study depicted a 2-year field trial in Brazil where soybean rust was responsible for 37–67% of soybean seed yield losses [1]. This study agreed with yield losses already observed in Asia, where the disease originates. Losses there can reach up to 80% [2]. Based on a disease risk assessment study conducted by Pivonia and Yang [3], climatic conditions in the soybean producing regions of the United States are suitable for similar yield losses. In 2009 (up to October), soybean rust has been detected in 14 states including 269 counties along the southeastern portion of the country (USDA Integrated Pest Management (IPM) web site; <http://sbr.ipmPIPE.org/cgi-bin/sbr/public.cgi>). So far, fungicide application has been effective in decreasing the severity of SR infection. However, there are only a few fungicides currently registered for foliar application on soybean in the United States. In

addition, fungicide application is expensive and does not always control the pathogen from the time of soybean flowering through pod fill. During this period the plant canopy is very dense; this can be an effective barrier to penetration of fungicides applied on top of the canopy. Scientists have screened over 1600 soybean accessions for resistance or tolerance to soybean rust (SR) [4,5]. Five resistance loci have been found (*Rpp1–Rpp5*) in five different accessions; however, none are present in soybean cultivars commercially grown in the United States. Moreover, there are many isolates of *P. pachyrhizi* and genes conferring resistance to all isolates have not been found. From this perspective, efforts should be focused on understanding the molecular mechanisms involved during infection, which is critical in identifying genes that could confer resistance.

The *P. pachyrhizi* life cycle is typical of the majority of other rust fungi (Fig. 1). *P. pachyrhizi* spores, named uredospores, are transported readily by air currents and can be disseminated hundreds of miles in just a few days. Once germination occurs, the uredospore produces a single germ tube (GT) that grows across the leaf surface until it reaches an appropriate surface where an appressorium (AP) forms. This penetration step occurs 7–12 h after the spore lands on the leaf adaxial surface. Appressoria form over anticlinal walls or over the center of epidermal cells, but rarely over stomata, in contrast to the habit of many other rusts. Thus, penetration is direct rather than through natural openings or through wounds in the leaf

* Corresponding author. Tel.: +1 301 504 5376; fax: +1 301 504 5728.

E-mail address: Arianne.Treblay@ars.usda.gov (A. Tremblay).

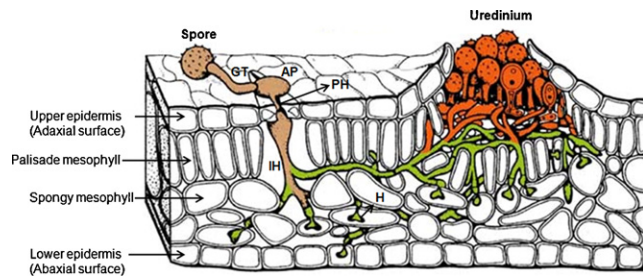


Fig. 1. Internal structure of a typical dicotyledon leaf showing the different cell layers and infection by a rust fungus. GT, germ tube; AP, appressorium; PH, penetration hyphae; IH, infection hyphae; H, haustorium. Schema was taken from Hahn (2000) [6].

tissue. Twenty hours after spore landing, penetration hyphae (PH), stemming from the appressorium cone, pass through the cuticle to emerge in the intercellular space where a septum is formed to produce the primary infection hypha (IH). Between 24 and 48 h after spore landing, the infection hypha grows between palisade cells to reach the spongy mesophyll cells where it forms the haustorium (H).

Once this first stage has been reached, 4 days after spore landing, additional hyphae emerge and spread through the entire spongy mesophyll layer of cells where many other haustoria are formed. At approximately 6 days after infection, some necrosis of epidermal cells occurs which is visible at the adaxial surface of the leaves as yellow mosaic discolorations (Fig. 2a). Hyphae aggregate and a uredinium arises in the spongy mesophyll cell layer. Uredinia can develop 6–8 days after spore landing and development might extend up to 4 weeks. The first uredospores produced by the uredinium emerge at the abaxial leaf surface 9–10 days after spore landing and spore production can be observed for up to 3 weeks. High rate of sporulation is typical of a susceptible reaction where lesions on the upper surface of the leaf are tan (Fig. 2b). Plants classified as resistant develop a dark, reddish-brown lesion with few or no spores (Fig. 2c) [7].

Few molecular and biological analyses have been done on the interaction between *P. pachyrhizi* and its soybean host. Since the discovery of the five resistance loci and their recent localization on the soybean genome, more work has been done to find new genes or alternative alleles involved in the resistance response of soybean against SR. Five hundred thirty more accessions showing different resistance responses have been screened using molecular markers. However, no new resistance genes were found [8]. In a different study, Calvo et al. found two soybean accessions possessing resistance to SR, which seems to be controlled by a recessive gene [9]. Chakraborty et al. found an alternative allele of *Rpp1*, named *Rpp1-b*, in a different accession. This allele seems to provide the soybean plant with broader resistance to multiple *P. pachyrhizi* isolates [10].

Since SR is an obligate biotroph, it is difficult to separate fungal cells from host cells. However, laser capture microdissection (LCM) offers a useful approach for isolating infected cells from non-infected cells. This eliminates contaminating background gene expression of non-infected cells. LCM has been used relatively recently in both plant and plant–pathogen interactions. Kerk et al. [11] successfully worked on different types of cells (parenchyma, hypocotyl, seedling petiole and procambium, mesophyll, bundle sheath, root meristem, stomatal, pavement, cotyledon procambium, shoot tip protoderm, leaf protoderm, shoot apical meristem and leaf primordium) from different plants (*Arabidopsis*, maize, radish, tomato and rice). Ramsay et al. [12] isolated giant cells from *Lycopersicon esculentum* plants infected by *Meloidogyne* spp., a root-knot nematode to analyze gene expression. An extensive study has been done on the interaction of the soybean cyst nematode, *Heterodera glycines*, with soybean plants using LCM, wherein nematode feeding sites (syncytia) were isolated from soybean roots. Expression levels in those roots were determined using EST and microarray analysis [13,14].

Microarray analysis combine with LCM of host–pathogen interactions can provide a broad view of genes, pathways and regulatory events involved in defense. Using soybean cv. Williams 82 infected by SR isolate MS06-1 between 168 and 240 hai, we found palisade and mesophyll cells with a brown coloration which had not been observed in non-infected plants. Moreover, palisade and mesophyll

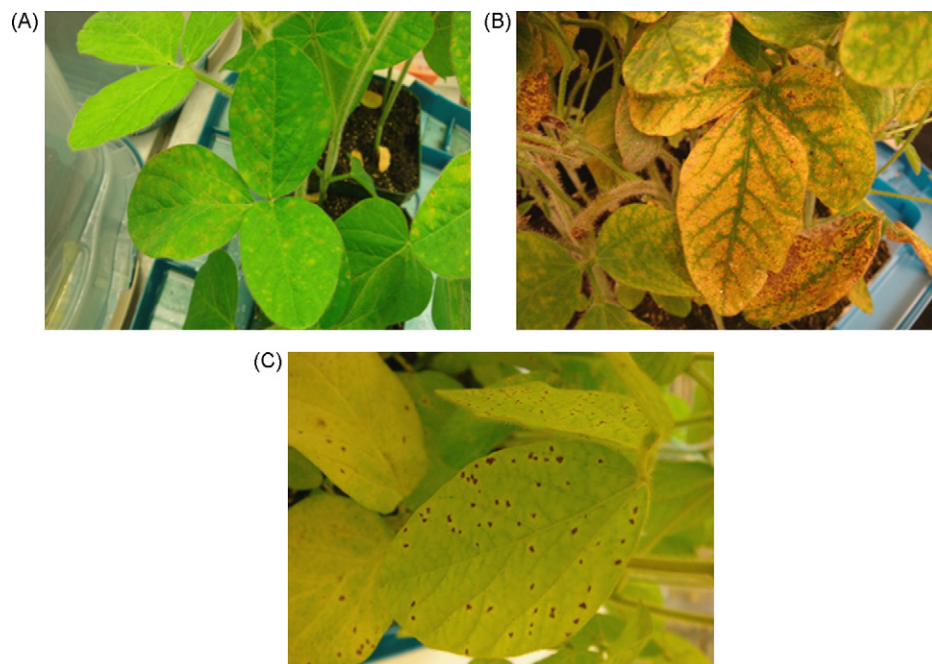


Fig. 2. SR symptoms observed on soybean leaves. (a) Yellow mosaic discoloration observed at 7 dai. (b) Tan lesions observed at 21 dai and (c) reddish-brown lesions observed at 14 dai. Photos were taken at the United States Department of Agriculture–Agricultural Research Service Stoneville Research Quarantine Facility in Mississippi. (For interpretation of the references to color in this figure legend, the reader is referred to the web version of the article.)

cells are the location where the vast majority of fungal infection structures developed. Therefore, we isolated these brown cells 10 days after infection (dai) using LCM. RNA was extracted, fluorescently labeled and hybridized to a soybean GeneChip® containing 37,744 *Glycine max* probe sets to study gene expression occurring within the palisade and mesophyll cells infected by SR. Microarray results identified sets of genes whose expression patterns show significant alterations in SR inoculated plants. The classification of these genes into functional categories and their putative roles will be discussed. Finally, analysis of gene expression was augmented through the overlay of our gene expression data on the extensive metabolic pathways provided in the Kyoto Encyclopedia of Genes and Genomes (KEGG) database [15].

2. Materials and methods

2.1. Pathogen isolation and plant inoculation

The *Phakopsora pachyrhizi* isolate (MS06-1) was obtained from urediniospores harvested from field-collected kudzu leaves in Jefferson County, Mississippi in August 2006. Its identity was confirmed by microscopy, enzyme-linked immunosorbent assay (ELISA) and polymerase chain reaction (PCR) as previously described [16]. Urediniospores were increased on a susceptible soybean cultivar, Williams 82 [17], at the Stoneville Research Quarantine Facility in Mississippi. The isolate was purified by picking a single uredinium using a fine needle under an Olympus SZX12 dissecting microscope and reinoculating it on leaves of Williams 82. This inoculation–isolation cycle was repeated four times. Urediniospores from this purified culture were harvested using a Cyclone Surface Sampler (Burkard Manufacturing Co. Ltd, UK) connected to a vacuum pump, beginning 10–14 (dai) and continuing at weekly intervals.

Inoculum was prepared using freshly collected urediniospores from Williams 82. Spore suspensions were made using sterile distilled water containing 0.01% Tween-20 (vol/vol), mixed, and filtered through a 100- μ m cell strainer (BD Biosciences, Bedford, MA) to remove any debris and clumps of urediniospores. Urediniospores were quantified using a hemocytometer and diluted to a final concentration of 1.1×10^5 spores/ml. Three plants (3-week-old seedlings of Williams 82) per 10 cm-pot with three replicates (pots) were inoculated. Inoculation was applied with Preval sprayer (Younkers, NY) at a rate of 1 ml of spore suspension per plant. The same solution minus spores was used for a mock inoculation on three pots of plants to monitor the infection. After inoculation, plants were placed in a dew chamber in the dark at 22 °C overnight (approximately 16 h) and then moved to Conviron growth chambers where temperatures were maintained at 23 °C during the day and 20 °C at night under a 16-h photoperiod with a light intensity of 280 μ E m⁻² s⁻¹. SR inoculated and mock-inoculated plants were kept in two different growth chambers.

2.2. Tissue procurement

For all replicates the first trifoliate of soybean was harvested 10 days after SR inoculation. The leaf tissue was cut into 1 cm square pieces and vacuum-infiltrated with Farmer's solution (FS) composed of 75% ethanol and 25% acetic acid [18] at room temperature for 1 h. Fresh FS was added to the samples and the tissue was incubated 12 h at 4 °C. The fixative was removed and leaves were dehydrated with a graded ethanol series (75%, 85%, 100%, 100%), 30 min each. Ethanol was replaced with 1:1 xylene:ethanol for 30 min, followed by three 100% xylene incubations (30 min each). Xylene was then replaced with paraffin by placing the specimens into a 58 °C oven and infiltrating the leaves sequentially in

25, 50 and 75% (1 \times) and 100% (3 \times) Paraplast + tissue embedding medium (Tyco Healthcare Group LP, Mansfield, MA) in each step for 3 h. Tissue was cast and mounted for sectioning. Serial sections of leaves were made on an American Optical 820 microtome (American Optical Co., Buffalo, NY) at a section thickness of 10 μ m. Serial sections were placed onto a pool of dH₂O made RNase-free with diethyl pyrocarbonate (DEPC) (Sigma, St. Louis, MO), on Leica PEN-Membrane 2.0 μ M membrane slides. Excess DEPC dH₂O was blotted and slides were allowed to dry. Slides were stored at 4 °C.

2.3. Laser capture microdissection

About one million square microns surface of palisade and mesophyll cells from infected and none infected leaves were collected by LCM 10 dai. Both LCM and archival image capture of microdissected SR infected leaves were performed on a Leica ASLMD microscope (Leica®, Germany). LCM cutting parameters varied; they were determined empirically for each session by examining how amenable the tissue was to LCM. However, cutting parameters for dissections performed with the 40 \times objective were approximately: power, 50; speed, 4; specimen balance, 4; offset, 30. Palisade-enriched tissue was collected from the slides in caps of PCR "SNAPSTRIP" 0.2 ml tubes (LabSource®, Willowbrook, IL).

2.4. RNA extraction and isolation

For microarray, RNA was extracted from each 1,000,000 μ m² of palisade and mesophyll cells (three replicates from each infected and non-infected samples) by micropipetting 20 μ l of XB buffer (Arcturus Bioscience Inc., Mountain View, CA) onto the tube cap. The tubes were centrifuged to collect liquid and sample at the bottom and incubated 30 min at 42 °C. RNA was isolated from the sample with the PicoPure RNA Isolation Kit (Arcturus®) according to the manufacturer's instructions, with the addition of a DNase treatment using DNA-free (Ambion®, Austin, TX) just before the second column wash. RNA yield was determined using the RNA 6000 Nano Assay® (Agilent Technologies®, Palo Alto, CA) on the Agilent 2100 Bioanalyzer® according to the manufacturer's instructions. RNA amplification of LCM samples was done with the GeneChip® Two-Cycle cDNA Synthesis Kit (Affymetrix®, Santa Clara, CA). Probe preparation and hybridizations were performed according to Affymetrix® guidelines at the Laboratory of Molecular Technology, SAIC-Frederick, Inc.; National Cancer Institute at Frederick, Frederick, MD, 21701, USA.

2.5. Microarray analyses

The GeneChip® Soybean Genome Array (Affymetrix®) was used for the microarray analyses. The high-density array is an 11-probe pair (25 bp per oligonucleotide), 11- μ feature size array, providing multiple independent measurements for each individual transcript. The array contains 37,744 *G. max* probe sets (35,611 transcripts). Thus, some redundancy is present. Details of the GeneChip® Soybean Genome Array can be obtained at (<http://www.affymetrix.com/index.affx>).

Affymetrix Genechips were imported and analyzed using the Mathworks MATLAB Bioinformatics Toolbox (Mathworks Inc., Natick, MA) where RMA normalization and log-2 expression values were calculated.

Volcano plots were produced using expression values with fold-changes of ≥ 2.0 and *p*-values ≤ 0.05 against the control. The *t*-test was used to calculate the resultant *p*-values. Additionally, such *p*-values underwent false-discovery analysis using Significance Analysis of Microarrays (SAM 3.0) with a false-discovery rate of 5%.

Table 1
PCR primer pairs used for quantitative PCR.

Probe set	Target gene product	Primer sequence	Temperature (°C)	Amplicon size (bp)
Gma.13457.1.S1_at	Anthranilate synthase, beta chain	Forward: TCCGAACCCCAATATCAACAG Reverse: CTATGCCTGCTTTGTCCCTG	65 °C	166
GmaAffx.91687.1.A1_s_at	Thioredoxin, nucleoredoxin and related proteins	Forward: AGGAGGACAAAGAAGGAAGCAA Reverse: CTAGGAGGGCGTTCACAATACTTC	65 °C	164
Gma.10620.1.S1_at	Glyoxylate/hydroxypyruvate reductase (D-isomer-specific 2-hydroxy acid dehydrogenase superfamily)	Forward: TGCAGGTTTGCCCAACTTCA Reverse: CCATCAGCACCCACATACAC	65 °C	144
GmaAffx.42586.1.A1_at	Predicted NUDIX hydrolase FGF-2 and related proteins	Forward: TGGGGATGATGTCATACGAACAC Reverse: CCTCGATCTAACAAAAGTGCCTG	65 °C	90
NA	Ubiquitin-3	Forward: GTCTAATGTTGGATGTGTTCCC Reverse: ACACAATTGAGTTCAACACAACCCG	65 °C	107

All annotations were obtained by performing BLASTX from the Affymetrix ID accession available at <http://affymetrix.com/index.affx>.

Pathways were generated using PAICE, a tool for coloring KEGG pathways given Enzyme Commission (EC) accessions (<http://paice.sourceforge.net>). PAICE was employed for its ability to handle duplicate gene-copies as well, color genes with large variances between time points, as well as color accessions given fold-change values. From this analysis, a total of 78 KEGG pathways were produced.

2.6. Confirmation of differential gene expression using quantitative PCR

For quantitative PCR, remaining RNA of both samples from microarray procedure was pooled together to give us about 19 ng of RNA. This RNA was used to generate first-strand cDNA. First-strand cDNA was synthesized using the SuperScript First-Strand Synthesis System for RT-PCR (Invitrogen) following the manufacturer's instruction using 0.08 mM of a modified oligo (dT) (5'CGTCATCTTGCGGCCGCAAGTCGT(10–14)30) and a second primer (5'TTCGGCTGCGAGAAGACGACTGAAGGGG3') to allow a subsequent amplification step by long distance (LD)-PCR [19]. Total cDNA was placed directly in a 50 µl volume PCR reaction with 1× high fidelity PCR buffer, 1.5 mM MgSO₄, 200 mM dNTPs, 300 nM final concentration primers (5'TTCGGCTGCGAGAAGACGACTGAAGGGG3' and 5'CGTCATCTTGCGGCCGCAAGTCGT3') and 1 unit of Platinum Taq Polymerase High Fidelity (Invitrogen). The cycling conditions consisted of the following steps: an initial 30 s denaturing step at 95 °C; 26 cycles at 95 °C for 15 s, 55 °C for 15 s, and 68 °C for 6 min; and a final extension of 72 °C for 10 min.

The expression patterns of four soybean genes expressed in our microarray dataset at time-zero and 10 dai were analyzed. A soybean housekeeping gene, ubiquitin-3 (Accession D28123) [20], was used to normalize the results. Other controls for Real-Time PCR had included reactions containing either no template or DNA processed with no reverse transcriptase.

PCRs using all primer sets were performed on three technical replicates. Real-Time PCR was performed using primers listed in Table 1. Relative quantities of gene expression were determined using the Stratagene Mx3000P Real-Time PCR system (Stratagene, La Jolla, CA) as described by the manufacturer. DNA accumulation during the reaction was measured with SYBR Green. The Ct (cycle at which there is the first clearly detectable increases in fluorescence)

values were calculated using software supplied with the Stratagene Mx3000P Real-Time PCR system. SYBR green dissociation curve of amplified products demonstrated the production of only one product per reaction. Data analysis was performed according to the sigmoidal model [21] to get absolute quantification, which is described in Tremblay et al. [22].

3. Results

3.1. Histology of *Phakopsora pachyrhizi* infection on *Glycine max* plants

Leaves of soybean cv. Williams 82 were inoculated with *P. pachyrhizi* isolate MS06-1 and grown for 10 days. A brown coloration in the palisade and mesophyll cells layers (Fig. 3a–b) was observed, most of the time close to an uredinium (Fig. 3c–d). Palisade and mesophyll cells showing brown coloration were collected by LCM.

3.2. Gene expression in palisade and mesophyll cells layer infected with SR as compared to non-infected

A total of 2982 genes were found to be significantly differentially expressed in palisade and mesophyll cells infected by SR (Supplementary data; Table S1), as compared to non-infected control plants. Out of the 2982 differentially expressed genes, 685 were induced, and 2297 were suppressed. There were 468 up-regulated genes that shared similarity with genes encoding known proteins, while 109 genes shared similarity with unknown proteins and 108 genes were not similar to other genes ($e\text{-value} \leq 10^{-2}$). The 50 most highly induced genes are listed in Table 2. Most of the up-regulated genes with similarity to genes encoding known proteins were related to defense and disease and metabolism functional categories (Fig. 4a). Genes encoding disease resistance-responsive proteins-related, stress-induced protein, class IV chitinases, thaumatin-like protein, osmotin and polyphenol oxidase are examples in the defense and disease category. Metabolic genes that were induced included caffeoyl-CoA 3-O-methyltransferase and chalcone synthase, which are both involved in the biosynthesis of phenylpropanoids (Fig. 5a).

There were 1670 down-regulated genes identified that share similarity with genes encoding known proteins (Supplementary data), while 401 down-regulated genes share similarity with unknown proteins and 226 genes share no similarity ($e\text{-value} \leq 10^{-2}$). The 50 most down-regulated genes are listed

Table 2List of the 50 most greatly induced and suppressed annotated genes in soybean cv. Williams 82 10 dai by SR (p -value ≤ 0.05).

Probe set	Gene annotation	Fold change	p -value
Up-regulated			
Gma.15636.2.S1.x.at	Hypothetical protein	621,3641	3.34E–03
Gma.3702.1.S1.at	Endochitinase PR4 precursor	492,6225	1.78E–05
Gma.17733.1.S1.s.at	Proteinase inhibitor I13, potato inhibitor I	458,2462	1.82E–03
Gma.6999.2.S1.s.at	Stress-induced protein SAM22	438,5823	1.84E–02
Gma.2821.1.S1.at	Osmotin	416,8519	5.87E–04
Gma.6999.1.S1.s.at	Stress-induced protein SAM22	408,975	2.12E–02
Gma.3734.1.S1.at	Proteinase inhibitor I13, potato inhibitor I	366,6009	2.03E–06
Gma.5574.1.S1.s.at	Pleiotropic drug resistance protein 12	335,8458	7.90E–06
Gma.6999.1.S1.x.at	Stress-induced protein SAM22	220,7037	5.89E–03
Gma.3713.1.S1.s.at	Aldo/keto reductase AKR	183,8092	1.64E–04
Gma.2593.1.S1.s.at	Glutathione S-transferase GST 15	182,1947	1.99E–03
Gma.772.1.S1.at	Hypothetical protein	143,0646	2.91E–03
Gma.5529.1.S1.at	NAD(P)H-dependent 6'-deoxychalcone synthase	133,782	3.47E–04
Gma.12045.1.S1.at	Asparagine synthetase 1	128,2755	2.36E–04
Gma.9397.1.S1.at	NHL3 (NDR1/HIN1-like 3)	125,3889	1.31E–04
Gma.16547.1.S1.at	WRKY86	116,8773	6.18E–03
Gma.6327.1.S1.s.at	B12D protein	114,4761	3.57E–04
Gma.5950.1.S1.s.at	Dirigent protein	107,7812	9.69E–04
Gma.10717.1.S1.a.at	Integral membrane family protein	105,524	1.34E–03
Gma.2096.1.S1.at	Protein At2g29340	104,1612	6.40E–03
Gma.3604.1.S1.at	Caffeoyl-CoA O-methyltransferase 1	93,3483	3.48E–05
Gma.5709.1.S1.at	Unknown protein	87,82372	3.22E–03
Gma.9947.1.S1.at	Hypothetical protein	84,40707	4.57E–05
Gma.16778.1.S1.at	VQ motif-containing protein	83,14188	9.56E–04
Gma.744.1.S1.at	WRKY transcription factor 41	77,94702	1.54E–04
Gma.4185.1.S1.at	ATEXLB1 (EXPANSIN-LIKE B1)	77,75584	1.21E–04
Gma.1654.1.S1.s.at	Coatomer protein complex, beta prime; beta'-COP protein	74,62076	6.37E–03
Gma.7559.1.S1.s.at	Polyphenol oxidase	72,6512	6.81E–05
Gma.16709.1.S1.s.at	Cytochrome P450 monooxygenase CYP82E13	67,80047	7.51E–05
Gma.15568.1.S1.at	Disease resistance-responsive protein-related/dirigent protein-related	66,93703	3.02E–04
Gma.2821.2.S1.a.at	Thaumatin-like protein	66,70191	1.14E–04
Gma.17802.1.S1.at	UVI1	63,02232	2.38E–04
Gma.17305.1.S1.at	Alpha-hydroxynitrile lyase	62,4359	6.62E–04
Gma.4375.1.S1.s.at	Cytosolic glutamine synthetase beta2	57,0043	1.10E–02
Gma.2523.1.S1.s.at	R 14 protein	50,31524	3.74E–05
Gma.1537.1.S1.at	Vesicle-associated membrane protein 725	50,03494	1.29E–03
Gma.8331.1.S1.at	Aldehyde dehydrogenase [Vitis	49,6297	4.32E–05
Gma.15664.1.S1.at	2'-hydroxydihydrodaidzein reductase	49,06484	1.95E–03
Gma.2821.2.S1.at	thaumatin-like protein	48,60514	1.67E–03
Gma.7728.1.S1.at	LacZ protein	48,01328	5.21E–03
Gma.8401.1.A1.at	Cytochrome P450 71D8	47,96981	1.20E–02
Gma.1748.1.S1.at	NAC domain protein NAC1	47,53361	7.79E–05
Gma.17594.1.A1.at	F1N19.23	47,12632	2.28E–04
Gma.2773.2.S1.at	F12P19.3	46,92901	1.86E–03
Gma.5129.1.S1.at	Pyridine nucleotide-disulphide oxidoreductase family protein	46,85986	6.14E–03
Gma.4483.1.S1.at	AMP-binding protein	46,33115	4.63E–03
Gma.17929.1.A1.at	Transferase	45,71365	7.56E–04
Gma.2578.1.S1.at	Endo-1,3-beta-glucanase	45,42094	7.39E–05
Gma.12031.2.S1.x.at	F17O7.4	45,19494	4.03E–04
Gma.8113.1.A1.at	No apical meristem (NAM) protein-like	44,89299	2.60E–03
Down-regulated			
Gma.10892.5.S1.at	Carbonic anhydrase	–929,314	3.74E–05
Gma.5294.1.S1.at	Gibberellin-regulated family protein	–624,912	1.70E–04
Gma.1379.2.A1.at	Gonadotropin, beta chain; Gibberellin regulated protein	–499,641	4.67E–07
Gma.10892.1.S1.a.at	Carbonic anhydrase	–498,86	3.15E–03
Gma.1201.1.A1.at	Hypothetical protein	–475,485	3.66E–04
Gma.3304.1.S1.at	Plant lipid transfer/seed storage/trypsin-alpha amylase inhibitor	–391,438	9.57E–05
Gma.11116.4.S1.at	Major intrinsic protein	–386,996	4.95E–03
Gma.3241.1.S1.a.at	Germin-like protein	–363,641	8.18E–04
Gma.11116.2.S1.at	Expressed protein	–342,63	7.59E–05
Gma.3208.2.S1.a.at	Oxalic acid oxidase	–241,535	3.50E–05
Gma.15007.1.A1.s.at	Ferredoxin [2Fe-2S], plant	–236,977	2.91E–03
Gma.15091.2.S1.at	Unknown protein	–232,571	2.90E–04
Gma.10591.2.S1.at	Glycine cleavage system H protein, mitochondrial precursor	–231,73	7.68E–05
Gma.1355.2.S1.s.at	Ribosomal protein L17 family protein	–230,499	2.62E–06
Gma.4575.1.S1.at	Fructose-bisphosphate aldolase	–226,442	4.97E–05
Gma.11254.2.S1.at	SAH7 protein	–224,213	7.74E–05
Gma.5294.1.S1.s.at	Gibberellin-regulated family protein	–213,993	2.91E–03
Gma.1992.1.S1.at	Hypothetical protein	–204,287	2.30E–04
Gma.3161.1.S1.at	Glutamine synthetase	–187,297	3.64E–03
Gma.17554.1.S1.a.at	Light harvesting chlorophyll a/b binding protein of PSII	–186,524	1.98E–04
Gma.4385.1.S1.s.at	Fasciclin-like arabinogalactan protein FLA2	–183,682	2.25E–04
Gma.10620.1.S1.at	NADH-dependent hydroxypyruvate reductase	–181,05	3.30E–04
Gma.10151.1.S1.at	thylakoid soluble phosphoprotein	–175,823	6.26E–04

Table 2 (Continued)

Probe set	Gene annotation	Fold change	p-value
Gma.2224.1.S1_s.at	Tubulin beta-1 chain	−175,601	3.82E−04
Gma.10771.1.A1_a.at	thiamin biosynthesis protein	−171,036	3.87E−05
Gma.15376.1.A1_s.at	Photosystem I reaction center subunit VI, chloroplast precursor	−170,931	2.21E−07
Gma.1160.1.S1.at	Ferritin-3, chloroplast precursor	−168,545	3.47E−04
Gma.289.1.S1_s.at	Ribulose biphosphate carboxylase small chains, chloroplast precursor	−161,412	8.10E−04
Gma.9720.1.S1.at	Transketolase, C-terminal-like	−155,611	9.19E−04
Gma.2503.1.S1.at	NADH-dependent hydroxypyruvate reductase	−151,021	6.79E−03
Gma.1955.4.S1_a.at	Chloroplast oxygen-evolving enhancer protein	−148,402	7.28E−03
Gma.11116.4.S1_s.at	Major intrinsic protein	−148,119	1.41E−04
Gma.10852.2.S1.at	Photosystem I reaction center subunit II, chloroplast precursor	−139,773	1.18E−03
Gma.15830.1.S1_s.at	Expressed protein	−137,618	4.19E−04
Gma.5785.1.S1.at	Endo-1,4-beta-glucanase/cellulase, putative	−135,82	2.89E−05
Gma.1791.1.S1.at	Ferredoxin-B	−135,768	6.15E−05
Gma.11034.1.S1.at	Oxygen-evolving enhancer protein 1, chloroplast precursor	−135,593	1.48E−02
Gma.289.1.S1_x.at	Ribulose biphosphate carboxylase small chains, chloroplast precursor	−135,508	5.62E−05
Gma.2360.1.S1.at	Light harvesting chlorophyll a/b binding protein of PSII	−134,651	2.92E−05
Gma.15462.1.S1_a.at	RNA-binding region RNP-1	−129,783	6.67E−03
Gma.3317.2.S1_a.at	Peroxisredoxin Q, putative	−128,673	3.86E−02
Gma.2360.3.S1.at	Light harvesting chlorophyll a/b binding protein of PSII	−124,514	2.60E−03
Gma.16678.1.S1.at	Chloroplast thioredoxin M-type	−124,044	7.86E−06
Gma.16829.1.S1_x.at	Nodulin-26	−123,956	1.99E−02
Gma.7309.2.S1_s.at	Glycolate oxidase	−122,753	2.71E−02
Gma.15620.1.S1.at	50S ribosomal protein L12, chloroplast precursor	−122,164	3.70E−04
Gma.15814.1.A1.at	Xyloglucan endotransglycosylase/hydrolase 16 protein	−121,095	1.97E−03
Gma.10771.3.S1_x.at	Thiamin biosynthesis protein	−118,366	8.00E−06
Gma.12822.1.S1.at	Cytochrome b6f complex subunit (petM), putative	−117,089	8.85E−04
Gma.14123.1.S1.at	Hypothetical protein	−116,114	4.56E−04

in Table 2. Most of the down-regulated genes with similarity to genes encoding known proteins were included in the metabolism and energy functional categories (Fig. 4b). Almost all genes included in these two categories encode enzymes involved in photosynthesis, such as chlorophyll A-B binding proteins (LHCA2, LHCB4.2, LHCB4.3, CAB, LHCA3.1, LHB1B1, LHB1B2, LHCB2.1, LHCB2.3, LHCB3, etc), photosystem I reaction center (sub-

unit II, III, psaK, PSI-N, V, VI, XI) and photosystem II proteins, ferredoxin proteins, and fructose-bisphosphate aldolase (Fig. 5b). Genes associated with carbon fixation metabolism were also affected. Transcripts encoding ribulose-bisphosphate carboxylase, ribulose-phosphate 3-epimerase, transketolase, sedoheptulose-bisphosphatase, fructose-bisphosphate aldolase, triosephosphate isomerase, glyceraldehyde-3-phosphate dehydrogenase, phospho-

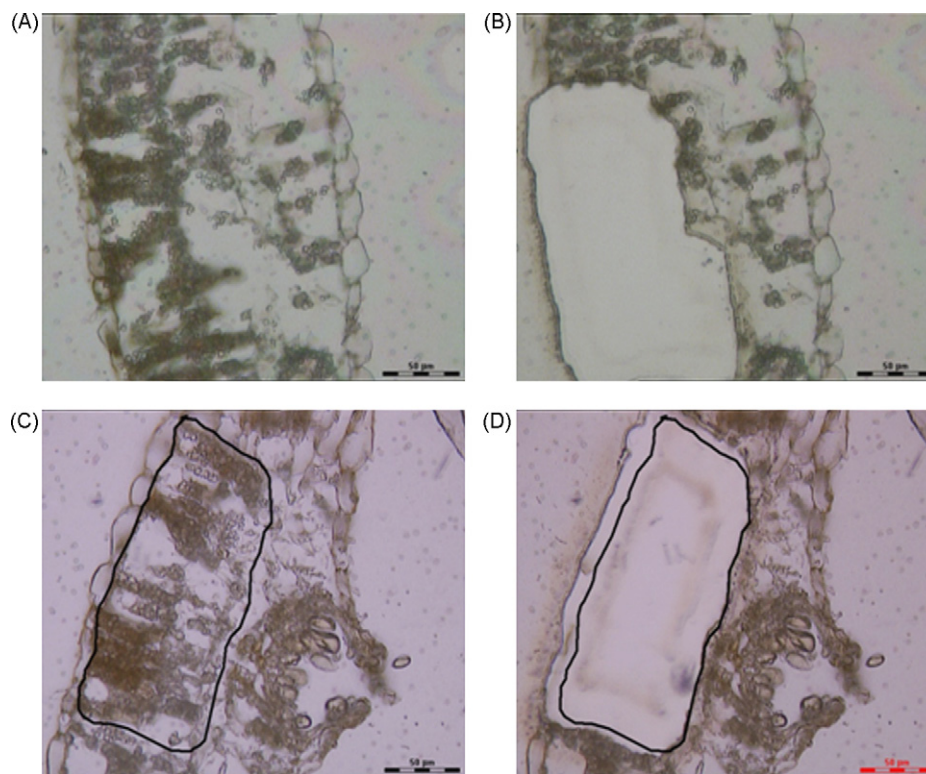


Fig. 3. LCM of palisade and mesophyll cells. (a) Longitudinal section of soybean leaf showing brown coloration inside the palisade and mesophyll cells before LCM. Magnification is 40 \times . (b) The same section after LCM with the microdissected palisade region absent from the section. (c) Longitudinal section of soybean leaf with a uridium (arrow) on the lower leaf surface before LCM (40 \times magnification). (d) The same section after LCM with the microdissected palisade and mesophyll region absent from the section. Scale bar represents 50 μ m at 40 \times .

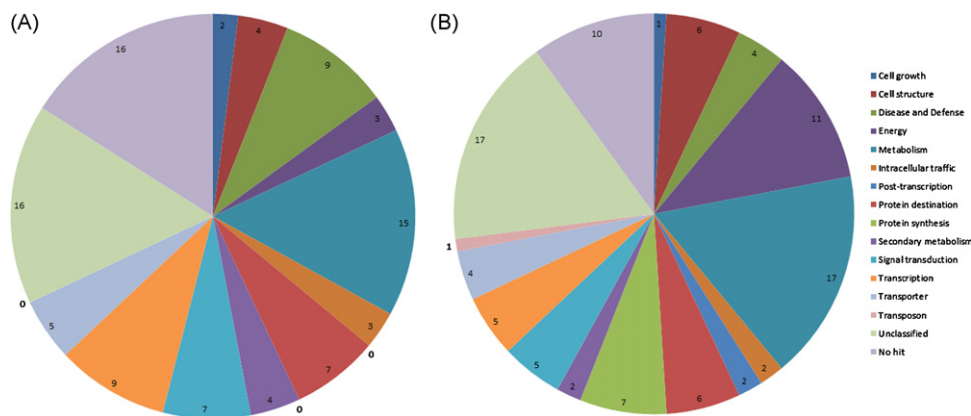


Fig. 4. Functional categorization of the probe sets (a) up (%) and (b) down-regulated (%) in soybean cultivar Williams 82 infected by SR 10 dai.

glycerate kinase, and carbonic anhydrase enzymes were all down-regulated (Fig. 5c).

Also, many genes encoding proteins involved in the pentose phosphate pathway were suppressed, such as transketolase, ribulose-phosphate 3-epimerase, ribose-phosphate pyrophosphokinase 1 and fructose-bisphosphate aldolase (Fig. 5d). There were numerous genes down-regulated that encode enzymes involved in nitrogen metabolism. Transcripts encoding nitrate reductase, nitrilase, glutamate synthase, glutamine synthase, and aminomethyltransferase were down-regulated (Fig. 5e). Genes involved in protein synthesis were also highly affected by SR infection. Many genes encoding ribosomal proteins were found to be down-regulated in our experiment including large subunit ribosomal protein L3, small subunit ribosomal protein S17 and many more (Fig. 5f). Table 3 lists all the enzymes found in the different pathways previously mentioned with their respective EC numbers.

3.3. Confirmation of differential gene expression by quantitative PCR

Quantitative PCR was conducted using four genes showing relatively high fold change in our microarray data. Although levels of expression were different between microarrays and quantitative PCR analysis, the trend of up or down-regulation was retained except for one gene (Table 4). The fold change was higher in microarray experiment compared to quantitative PCR. Differences at the level of expression between these two methods have been reported previously in numerous studies [20,23].

4. Discussion

Our study focused on using a highly infectious isolate of SR on a susceptible soybean cultivar to gain a better understanding of what is happening to the plant during the infection process. Palisade and mesophyll cells showing a brown coloration at 10 dai were collected by LCM to study soybean gene expression at this specific location and time using microarrays. A total of 380 genes were up-regulated and 1640 genes were down-regulated.

Panthee et al. identified genes that might be involved in a defense response against *P. pachyrhizi* by soybean cv. 5601 T plants 72 h after infection (hai) using microarrays [24]. Most of the induced genes had defense- and stress-related functions such as genes encoding an SA-related protein, heat shock protein (HSP), a leaf senescence-associated receptor-like kinase, a glutathione S-transferase (GST), and chalcone synthase. A more extensive list of candidate genes that regulate or affect soybean defense mechanism or are involved in mediating the successful establishment of SR in soybean plants was reported by van de Mortel et al. [19]. They

examined a resistant and a susceptible soybean cultivar at different time-points during the infection using whole leaf tissue. They found that there is a first burst of soybean gene expression at the beginning of the infection (6–12 hai), followed by a decline in expression of these same genes, followed by a subsequent rise back to high expression levels after 72 h in the resistant plants and later in the susceptible plants. Genes from the flavonoid biosynthetic pathway and WRKY transcription factor family, which are involved or associated with plant defense and stress responses, followed this pattern. If we compare our study resulting from laser capture microdissected tissues to the study of van de Mortel et al. [19] using whole leaves of susceptible Empraba-48 genotype at 7 dai, we find that out of our 380 up-regulated genes, 75 identified in infected leaf tissue by van de Mortel et al. [19] as well, while 305 genes were unique, identify in only our experiment which focused on gene expression at the specific infection site, the uredinium. All genes classified in our dataset as related to cell growth and division and intracellular traffic functional categories were unique. Eighty percent of genes we identified as members of the energy category were unique including phosphoenolpyruvate (PEP) carboxylase. About 75% of our genes included in cell structure, protein destination and transcription categories were unique to our experiment. Finally, 58% of our genes classified as involved in signal transduction were unique to our LCM isolated material. Out of 1640 down-regulated genes identified in our experiment, 1601 were unique as compared to the results of van de Mortel et al. [19]. Of the 39 genes in common with those identified by van de Mortel et al. [19] were triosephosphate isomerase and transketolase involved in carbon fixation and many 50S ribosomal proteins.

During an infection, a lot of changes occur in the host plant tissues [25]. The first major change consists of a decrease in the rate of photosynthesis correlated with an increase in the area of infected tissues. When broad beans are infected by rust and sugar beets by powdery mildew [26], chloroplasts lose their structural integrity due to an inhibition in photosynthetic CO₂ assimilation. This change in the chloroplast ultrastructure corresponds to a reduction in the capacity for sucrose production. Early in the infection process of leaves by rust, the photosynthetic rate is unaltered; after sporulation there is a decrease in the ability of the plant to fix carbon, which seems to be related to the destruction of the chloroplasts, the degradation and the loss of chlorophyll concentration. The infection of the plant causes a block in the non-cyclic electron transport chain by reducing the amount of cytochromes without affecting the integrity of the photosystems I and II. Indeed, our results show that photosynthesis in soybean leaves is highly affected 10 dai by SR. Numerous genes encoding enzymes involved in photosynthesis are suppressed compared to the uninfected plant. These results are in agreement with Polesani et al., who studied transcriptome changes

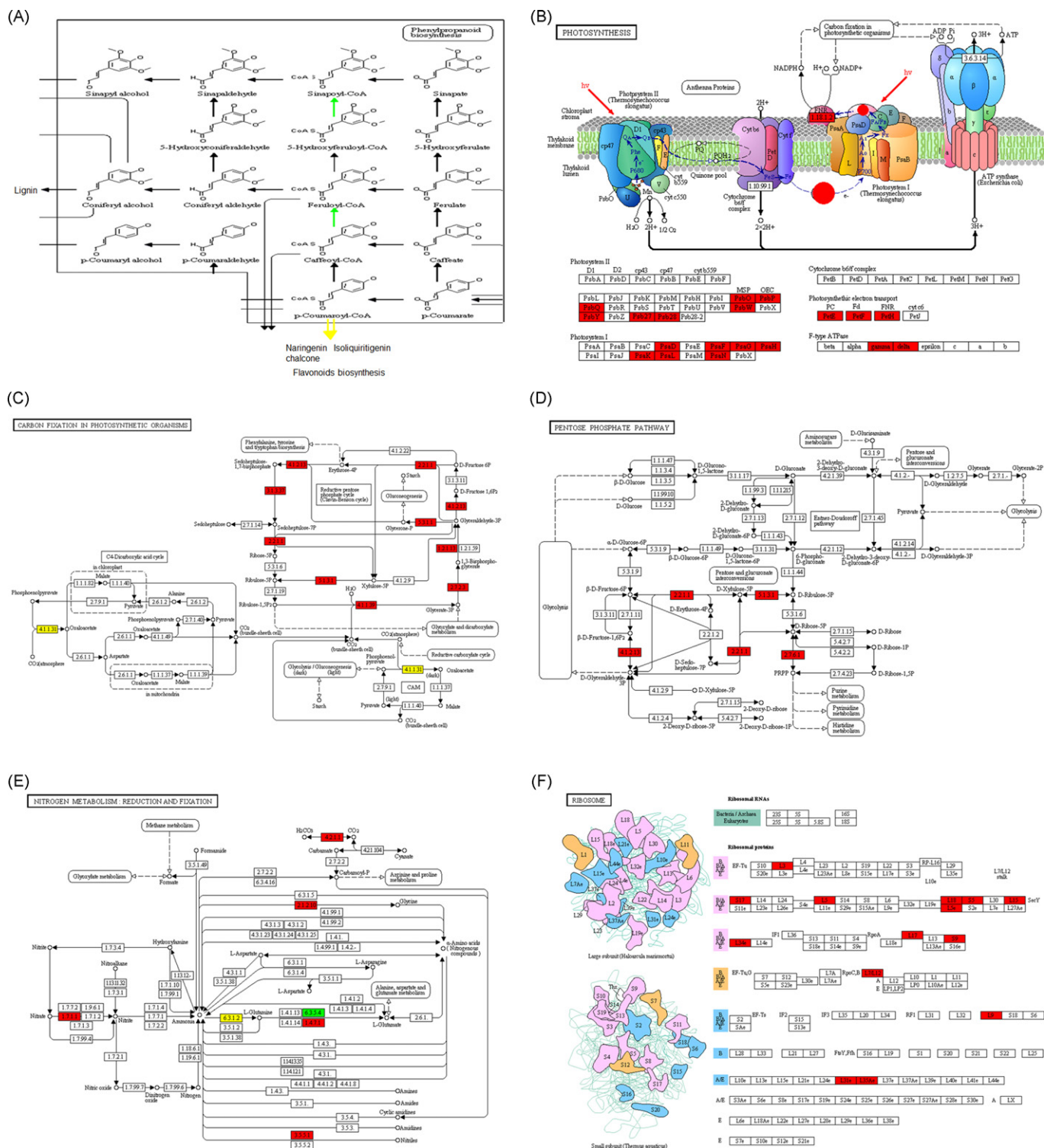


Fig. 5. Expression profiles of the RNAs encoding enzymes in different metabolic pathways. (a) Biosynthesis of phenylpropanoids, (b) photosynthesis, (c) carbon fixation of photosynthetic organisms, (d) pentose phosphate, (e) nitrogen metabolism and (f) ribosome pathways. The expression level of each RNA is associated with a specific color. Enzymes colored in red are up-regulated, the ones colored in green are down-regulated and the ones colored in yellow indicates that this specific RNA encodes for different forms of the same enzyme and those different copies are up or down-regulated. (For interpretation of the references to color in this figure legend, the reader is referred to the web version of the article.)

in grapevine infected by *Plasmopara viticola* causing mildew [27]. The most striking transcriptional down-regulation in grape leaves infected with mildew was observed in genes involved in photosynthesis e.g. chlorophyll a-b binding proteins and photosystem components, consistent with a measurable reduction in chlorophyll content during pathogenesis. Transcriptional down-regulation of

photosynthesis-related genes has been reported previously also during compatible interactions between potato and *P. infestans* [28] and between soybean and *P. sojae* [29].

In botany by definition, an obligate parasite must have a living (green) plant to survive. It cannot survive by consuming dead or dying organic matter. So, even if most of the changes occurring

Table 3

Enzymes involved in different metabolic pathways, for which their respective RNAs were found to be down-regulated in our microarray dataset.

Enzyme name	KEGG EC number	Probe set
Photosynthesis		
Ferredoxin–NADP ⁺ reductase	1.18.1.2	Gma.3305.1.S1.at
F-type H ⁺ -transporting ATPase subunit a	3.6.3.14	Gma.10788.1.S1.at
Carbon fixation in photosynthetic organisms		
Fructose-bisphosphate aldolase, class I	4.1.2.13	Gma.10990.2.S1.x.at
Transketolase	2.2.1.1	Gma.9720.1.S1.at
Fructose-1,6-bisphosphatase II/sedoheptulose-1,7-bisphosphatase	3.1.3.37	Gma.2026.1.S1.at
Triosephosphate isomerase (TIM)	5.3.1.1	Gma.10722.1.S1.at
Glyceraldehyde-3-phosphate dehydrogenase (NADP ⁺) (phosphorylating)	1.2.1.13	Gma.13868.1.S1.at
Ribulose-phosphate 3-epimerase	5.1.3.1	Gma.6333.3.S1.at
Phosphoglycerate kinase	2.7.2.3	Gma.17433.1.S1.at
Ribulose-bisphosphate carboxylase large chain	4.1.1.39	Gma.289.1.S1.s.at
Phosphoenolpyruvate carboxylase	4.1.1.31	Gma.12444.1.S1.at
Pentose phosphate		
Transketolase	2.2.1.1	Gma.9720.1.S1.at
Ribulose-phosphate 3-epimerase	5.1.3.1	Gma.6333.3.S1.at
Fructose-bisphosphate aldolase, class I	4.1.2.13	Gma.10990.2.S1.x.at
Ribose-phosphate pyrophosphokinase	2.7.6.1	Gma.7021.2.A1.a.at
Nitrogen metabolism		
Carbonic anhydrase	4.2.1.1	Gma.10892.1.S1.a.at
Aminomethyltransferase	2.1.2.10	Gma.2009.1.S1.at
Nitrate reductase (NADH)	1.7.1.1	Gma.8416.1.S1.at
Glutamate synthase (ferredoxin)	1.4.7.1	Gma.1390.1.S1.at
Nitrilase	3.5.5.1	Gma.16036.1.A1.at
Glutamine synthetase	6.3.1.2	Gma.3161.1.S1.at
Asparagine synthase (glutamine-hydrolysing)	6.3.5.4	Gma.12045.1.S1.at

inside the infected plants are in favor of the fungus since it draws all of its nutrition from the green plant, the soybean plant succeeds in staying alive. Within an infected leaf, there are uninfected cells that still perform photosynthesis and may be able to compensate for the decrease in photosynthesis of infected cells. For example, in pustules formed on bluebell leaves by the rust *Uromyces muscari*, chlorophyll was lost and other changes also occurred, suggesting that non-cyclic electron transport was reduced in those infected tissues, but the level of photosynthesis was apparently unaltered between pustules [30,31].

The second major change consists of the uncoupling of oxidative phosphorylation in the chloroplast. This uncoupling prevents ATP synthesis via the electron transfer chain and favors the accumulation of ADP and the increase in rate of oxygen uptake. This increase in the rate of respiration is probably due to the presence of respiring fungal tissues producing diffusible substances or toxins. Such increased respiratory levels lead to the rapid depletion of the plants carbohydrate reserves. Since there is less carbohydrate available for production of ATP molecules, an increase in pentose phosphate metabolism is needed. This is what is seen in some plant–fungal interactions such as rice infected by the sheath blight fungus, *Rhizoctonia solani* [32]. In this case, the PEP carboxylase is down-regulated. However in our experiment, we observed a complete shutdown of the pentose phosphate metabolism as well as most of the other pathways of carbohydrate metabolism that produce ATP, including the tricarboxylic acid (TCA) cycle, starch and sucrose metabolism, galactose metabolism, inositol phosphate metabolism, glycolysis, and the pentose phosphate pathway. Some

of energy required by plants for respiration is probably coming from the conversion of lactate to pyruvate by lactate dehydrogenase. Pyruvate goes to the TCA cycle to produce ATP molecules needed. This alternative way of producing ATP molecules is highlighted in our study by the upregulation of some enzymes involved in the pyruvate metabolism.

Pentose phosphate metabolism is the main pathway for production of phenolic compounds, which are responsible for the activation of defense mechanisms. Our results suggest that pentose phosphate metabolism is down-regulated during SR infection which agrees with the fact that susceptible plant don't succeed to build an efficient defense mechanism. However, we found that many genes encoding enzymes involved in the biosynthesis of phenylpropanoids are up-regulated. Also, the gene encoding PEP carboxylase was up-regulated in our experiment; this enzyme can convert 3-dehydroshikimate to p-coumarate, which is the substrate driving the production of phenylpropanoid compounds.

Other genes encoding proteins involved in plant defense were up-regulated, but no defense pathway appeared to be completely activated at the transcript level. We found induction of the genes encoding β -1,3-glucanase, glutathione S-transferase and the pathogenesis-related protein 10 (PR-10), all of which are induced by salicylic acid (SA), which is produced in response to pathogen infection [33,34,35]. However, no genes encoding enzymes necessary for synthesis of SA were noted as induced. Other genes, such as those encoding polyphenol oxidase and cysteine protease inhibitor, which are induced following jasmonic acid (JA) synthesis [36,37,38,39], were also induced, as were genes encoding

Table 4

Confirmation of differential gene expression base on microarray using quantitative PCR.

Probe set	Gene description	Fold change	
		Microarray	Quantitative PCR
Gma.13457.1.S1.at	Anthranilate synthase, beta chain	–18	–0.8
GmaAffx.91687.1.A1.s.at	Thioredoxin, nucleoredoxin and related proteins	10	1.5
Gma.10620.1.S1.at	Glyoxylate/hydroxypyruvate reductase (D-isomer-specific 2-hydroxy acid dehydrogenase superfamily)	–181	4
GmaAffx.42586.1.A1.at	Predicted NUDIX hydrolase FGF-2 and related proteins	243	3

12-oxophytodienoate reductase and allene oxide synthase (AOS), enzymes involved in JA production. However, phospholipase A2 and lipoxygenase 2 were suppressed. A gene encoding chitinase IV was up-regulated as were genes encoding chitinase proteins, well known as digestive enzymes that break down glycosidic bonds in chitin which comprise the cell wall of fungi. They are also induced following JA synthesis [40,41]. However, induction of all these genes is not sufficient to elicit an effective defense response against SR in this susceptible soybean cultivar, but it is apparent that the plant continues to fight the infection process by expressing defense-related genes.

One condition that contributes to the rust infection on grasses is low nitrogen levels in the soil [42,43]. By shutting down nitrogen metabolism, the fungus improves its ability to infect. Indeed, a decrease in nitrate reductase activity has been observed by Sadler and Scott [44] during the first 2 days of infection of barley leaves by *Erysiphe graminis*. However, most studies report that nitrogen assimilation increases after this early stage of infection [45,46,47]. Van de Mortel et al. [19] demonstrated that there is a biphasic change in mRNA in response to SR infection, that there is an increase in levels of transcripts encoding enzymes involved in nitrogen metabolism after 24 hai, then a decrease at 10 dai as we saw in our experiment. However, in our experiment the transcript encoding asparagine synthase, also involved in nitrogen metabolism had a different expression profile at 10 dai, its expression increases. Asparagine synthase activity has been reported to increase in barley leaves infected by *E. graminis* at later stages of infection [44]. However, in barley other enzymes (NAD⁺ glutamate dehydrogenase, NADP⁺ glutamate dehydrogenase and glutamine synthase) involved in nitrogen assimilation were also increased. In our case, with soybean, asparagine synthase expression could ultimately be used to produce alanine, a precursor of pyruvate which would allow the soybean leaves infected with SR to produce ATP via the TCA cycle.

Many studies on biotrophic interaction between a fungus and its host plant show that translational activity as well as ribosomal biogenesis is reduced at the early stage of infection reflecting a major change in gene translation [48,49,50,51,52]. Yamamoto et al. [53] demonstrated that this reduction in protein synthesis is really specific to the early stage of infection up to 3 dai. After 3 dai, protein synthesis increases [54]. On the other hand, Polesani et al. showed at the latest stage of infection of grapevine with *Plasmopara viticola*, that genes involved in protein metabolism are predominantly repressed suggesting a repression of protein synthesis and turnover [27]. These results are in agreement with our data which show a down-regulation of protein synthesis at 10 dai.

These results indicate that there are many different changes occurring between 7 and 10 dai in a susceptible soybean plant infected by SR. Some changes have already been seen in other fungi including other rusts but many changes seem to be specific to SR. This experiment also provides new information about the infection process. It provides insight into the needs of the pathogen and what genes are required and not needed for the pathogen to sporulate. For example, the reduction in nitrogen metabolism and protein synthesis that occurs in the plant at the end of the infection process may be an important trigger for sporulation of the fungus. Zuk et al. [55] found that a repression of 14-3-3 proteins, well known for their interaction with other proteins, affect nitrogen fixation by regulating nitrate reductase (NR). Since NR is a key enzyme in amino acid metabolism, they found that a repression in these 14-3-3 proteins also affects protein content by boosting it. Presence of 14-3-3 proteins in all eukaryotes including soybean cells provides an advantage to use these proteins to up-regulate instead of down-regulate nitrogen metabolism and protein synthesis at 10 dai with ASR and perhaps stop the fungus sporulation and its spread into the environment. This experiment gives us a better understanding

of gene expression in the fungus during the sporulation cycle that may help us to identify approaches to broaden the resistance of soybean to SR. Furthermore, it expands our knowledge about the development of this new exotic pathogen that threatens soybean production.

Acknowledgments

The authors thank Dr. Jeannine Rowland and Syra Sikandar for critical reading and editing of the manuscript. The authors greatly appreciate the continued support provided by the United Soybean Board under grant 8254. Mention of trade names or commercial products in this article is solely for the purpose of providing specific information and does not imply recommendation or endorsement by the United States Department of Agriculture. Technical assistance for the Affymetrix® array hybridizations and data acquisition was provided by Dr. David Munroe and Nicole Lum at the Laboratory of Molecular Technology, SAIC-Frederick, National Cancer Institute at Frederick, Frederick, Maryland 21701, USA. Data are available soon through the web site <http://bioinformatics.towson.edu/SGMD3/>.

Appendix A. Supplementary data

Supplementary data associated with this article can be found, in the online version, at doi:10.1016/j.plantsci.2010.04.011.

References

- [1] S. Kumudini, C.V. Godoy, J.E. Board, J. Omielan, M. Tollenaar, Mechanisms involved in soybean rust-induced yield reduction, *Crop Sci.* 48 (2008) 2334–2342.
- [2] M.R. Miles, R.D. Frederick, G.L. Hartman, Soybean rust: is the U.S. soybean crop at risk? (2003). APS net available: <http://www.apsnet.org/online/feature/rust/>.
- [3] S. Pivonia, X.B. Yang, Assessment of epidemic potential of soybean rust in the United States, *Plant Dis.* 89 (2005) 678–682.
- [4] M.R. Miles, R.D. Frederick, G.L. Hartman, Evaluation of soybean germplasm for resistance to *Phakopsora pachyrhizi*, *Plant Health Prog.* (2006). Available: <http://www.plantmanagementnetwork.org/php/> (doi:10.1094/PHP-2006-0104-01-RS).
- [5] M.R. Miles, W. Morel, J.D. Ray, J.R. Smith, R.D. Frederick, et al., Adult plant evaluation of soybean accessions for resistance to *Phakopsora pachyrhizi* in the field and greenhouse in Paraguay, *Plant Dis.* 92 (2008) 96–105.
- [6] M. Hahn, The rust fungi. Cytology, physiology and molecular biology of infection, in: J. Kronstadt (Ed.), *Fungal Pathology*, Kluwer Academic Publisher, Dordrecht, 2000, pp. 267–306.
- [7] E.E. Hartwig, K.R. Bromfield, Relationships among three genes conferring specific resistance to rust in soybeans, *Crop Sci.* 23 (1983) 237–239.
- [8] J.D. Ray, W. Morel, J.R. Smith, R.D. Frederick, M.R. Miles, Genetics and mapping of adult plant rust resistance in soybean PI 587886 and PI 587880A, *Theor. Appl. Genet.* 119 (2009) 271–280.
- [9] É.S. Calvo, R.A.S. Kiihl, A. Garcia, A. Harada, D.M. Hiromoto, Two major recessive soybean genes conferring soybean rust resistance, *Crop Sci.* 48 (2008) 1350–1354.
- [10] N. Chakraborty, J. Curley, R.D. Frederick, D.L. Hyten, R.L. Nelson, et al., Mapping and confirmation of a new allele at *Rpp1* from soybean PI 594538A conferring RB lesion-type resistance to soybean rust, *Crop Sci.* 49 (2009) 783–790.
- [11] N. Kerk, T. Ceserani, S.L. Tausta, I. Sussex, T. Nelson, Laser-capture microdissection of cells from plant tissues, *Plant Physiol.* 132 (2003) 27–35.
- [12] K. Ramsay, Z. Wang, M.G.K. Jones, Using laser capture microdissection to study gene expression in early stages of giant cells induced by root-knot nematodes, *Mol. Plant Pathol.* 5 (2004) 587–592.
- [13] V.P. Klink, B.F. Matthews, Developing a systems biology approach to study disease progression caused by *Heterodera glycines* in *Glycine max*, *Gene Regul. Sys. Biol.* 2 (2007) 1–17.
- [14] V.P. Klink, N. Alkharouf, M. MacDonald, B. Matthews, Laser capture microdissection (LCM) and expression analyses of *Glycine max* (soybean) syncytium containing root regions formed by the plant pathogen *Heterodera glycines* (soybean cyst nematode), *Plant Mol. Biol.* 59 (2005) 965–979.
- [15] M. Kanehisa, S. Goto, S. Kawashima, Y. Okuno, M. Hattori, The KEGG resource for deciphering the genome, *Nucleic Acids Res.* 32 (2004) D277–D280.
- [16] S. Li, W.F. Moore, B.L. Spinks, B.C. Wells, G.L. Sciumbato, et al., Occurrence of Asian soybean rust caused by *Phakopsora pachyrhizi* in Mississippi, *Plant Health Prog.* (2007). Available: <http://www.plantmanagementnetwork.org/php/> (doi:10.1094/PHP-2007-0917-02-BR).

- [17] D.L. Hyten, J.R. Smith, R.D. Frederick, M.L. Tucker, Q. Song, et al., Bulk segregant analysis using the GoldenGate assay to locate the *Rpp3* locus that confers resistance to soybean rust in soybean, *Crop Sci.* 49 (2009) 265–271.
- [18] J.E. Sass, Botanical Microtechnique, Iowa State College Press, Ames, 1958.
- [19] M. van de Mortel, J.C. Recknor, M.A. Graham, D. Nettleton, J.D. Dittman, et al., Distinct biphasic mRNA changes in response to Asian soybean rust infection, *Mol. Plant Microbe Interact.* 20 (2007) 887–899.
- [20] L.A. Peterson, M.R. Brown, A.J. Carlisle, E.C. Kohn, L.A. Liotta, et al., An improved method for construction of directionally cloned cDNA libraries from microdissected cells, *Cancer Res.* 58 (1998) 5326–5328.
- [21] R.G. Rutledge, D. Stewart, A kinetic-based sigmoidal model for the polymerase chain reaction and its application to high-capacity absolute quantitative real-time PCR, *BMC Biotechnol.* 8 (2008) 47.
- [22] A. Tremblay, S. Li, B.E. Scheffler, B.F. Matthews, Laser capture microdissection and expressed sequence tag analysis of uredinia formed by *Phakopsora pachyrhizi*, the causal agent of Asian soybean rust, *Physiol. Mol. Plant Pathol.* 73 (2009) 163–174.
- [23] N. Ithal, J. Recknor, D. Nettleton, L. Hearne, T. Maier, et al., Parallel genome-wide expression profiling of host and pathogen during soybean cyst nematode infection of soybean, *Mol. Plant Microbe Interact.* 20 (2007) 293–305.
- [24] D.R. Panthee, J.S. Yuan, D.L. Wright, J.J. Marois, D. Mailhot, et al., Gene expression analysis in soybean in response to the casual agent of Asian soybean rust (*Phakopsora pachyrhizi* Sydow) in an early growth stage, *Funct. Integr. Genomics* 7 (2007) 291–301.
- [25] S. Isaac, Fungal-plant interactions, *Q. Rev. Biol.* 68 (3) (1993), doi:10.1086/418217 (Published in Association with Stony Brook University, University of Chicago Press).
- [26] J.F. Farrar, D.H. Lewis, Nutrient relations in biotrophic infections, in: G.F. Pegg, P.G. Ayres (Eds.), *Fungal Infection of Plants*, Cambridge University Press, Cambridge, 1987, pp. 92–132.
- [27] M. Polesani, F. Desario, A. Ferrarini, A. Zamboni, M. Pezzotti, et al., cDNA-AFLP analysis of plant and pathogen genes expressed in grapevine infected with *Plasmopara viticola*, *BMC Genomics* 9 (2008) 142–156.
- [28] P. Moy, D. Qutob, B.P. Chapman, I. Atkinson, M. Gijzen, Patterns of gene expression upon infection of soybean plants by *Phytophthora sojae*, *Mol. Plant Microbe Interact.* 17 (2004) 1051–1062.
- [29] S. Restrepo, K.L. Myers, O. del Pozo, G.B. Martin, A.L. Hart, et al., Gene profiling of a compatible interaction between *Phytophthora infestans* and *Solanum tuberosum* suggests a role for carbonic anhydrase, *Mol. Plant Microbe Interact.* 18 (2005) 913–922.
- [30] J.D. Scholes, J.F. Farrar, Photosynthesis and chloroplast functioning within individual pustules of *Uromyces muscari* on bluebell leaves, *Physiol. Mol. Plant Pathol.* 27 (1985) 387–400.
- [31] B.B. Buchanan, S.W. Hutcheson, A.C. Magyarosy, P. Montallini, Photosynthesis in healthy and diseased plants, in: P.G. Ayres (Ed.), *Effect of Disease on the Physiology of the Growing Plant*, Cambridge University Press, Cambridge, 1981, pp. 13–28.
- [32] J. Danson, K. Wasano, A. Nose, Infection of rice plants with the sheath blight fungus causes an activation of pentose phosphate and glycolytic pathways, *Eur. J. Plant Pathol.* 106 (2000) 555–561.
- [33] T.P. Delaney, S. Uknes, B. Vernooij, L. Friedrich, K. Weymann, et al., A central role of salicylic acid in plant disease resistance, *Science* 266 (1994) 1247–1250.
- [34] A.M. Murphy, L.J. Holcombe, J.P. Carr, Characteristics of salicylic acid-induced delay in disease caused by a necrotrophic fungal pathogen in tobacco, *Physiol. Mol. Plant Pathol.* 57 (2000) 47–54.
- [35] Y. Narusaka, M. Narusaka, T. Horio, H. Ishii, Comparison of local and systemic induction of acquired disease resistance in cucumber plants treated with benzothiadiazoles or salicylic acid, *Plant Cell Physiol.* 40 (1999) 388–395.
- [36] C.A. Ryan, Protease inhibitors in plants: genes for improving plant defenses against insects and pathogens, *Annu. Rev. Phytopathol.* 28 (1990) 425–429.
- [37] J.S. Thaler, M.J. Stout, R. Karban, S. Duffey, Jasmonate-mediated induced plant resistance affects a community of herbivores, *Ecol. Entomol.* 26 (2001) 312–324.
- [38] E.E. Farmer, C.A. Ryan, Inter-plant communication: airborne methyl jasmonate induces synthesis of proteinase inhibitors in plant leaves, *Proc. Natl. Acad. Sci. USA* 87 (1990) 7713–7717.
- [39] E.E. Farmer, R.R. Johnson, C.A. Ryan, Regulation of expression of proteinase inhibitor genes by methyl jasmonate and jasmonic acid, *Plant Physiol.* 98 (1992) 995–1002.
- [40] J.M. Davis, H. Wu, J.E. Cooke, J.M. Reed, K.S. Luce, et al., Pathogen challenge, salicylic acid, and jasmonic acid regulate expression of chitinase gene homologs in pine, *Mol. Plant Microbe Interact.* 15 (2002) 380–387.
- [41] R. Rakwal, G. Yang, S. Komatsu, Chitinase induced by jasmonic acid, methyl jasmonate, ethylene and protein phosphatase inhibitors in rice, *Mol. Biol. Rep.* 31 (2004) 113–119.
- [42] N. Doubrava, J. Blake, Leaf disease of lawns, Clemson Cooperative Extension, HGIC 2152, 1999 3 pp. Available: <http://www.clemson.edu/extension/hgic/>.
- [43] A. Hagan, Leaf spot and rust diseases of turfgrasses, Alabama Cooperative Extension System, ANR-621, 2005, 6 pp. Available: www.aces.edu.
- [44] R. Sadler, K.J. Scott, Nitrogen assimilation and metabolism in barley leaves infected with the powdery mildew fungus, *Physiol. Plant Pathol.* 4 (1974) 235–247.
- [45] F.T. Last, Analysis of the effects of *Erysiphe graminis* D.C. on the growth of barley, *Ann. Bot. N. S.* 26 (1962) 279–289.
- [46] J.F. Jenkin, Nitrogen and leaf diseases of spring barley, in: *Fertilizer Plant Use and Plant Health*, International Potash Institute, Berne, Switzerland, 1977, pp. 119–128.
- [47] D.R. Walters, N.D. Paul, P.G. Ayres, Effects of mildew and nitrogen on grain yield of barley artificially infected in the field, *Ann. Bot.* 53 (1984) 145–148.
- [48] M.J.R. Mould, M.C. Heath, Ultrastructural evidence of differential changes in transcription, translation, and cortical microtubules during in planta penetration of cells resistant or susceptible to rust infection, *Physiol. Mol. Plant P.* 55 (1999) 225–236.
- [49] M.C. Heath, Signaling between pathogenic rust fungi and resistant or susceptible host plants, *Ann. Bot.* 80 (1997) 713–720.
- [50] J.M. Manners, K.J. Scott, Translational activity of polysomes of barley leaves during infection by *Erysiphe graminis f.sp. hordei*, *Phytopathology* 73 (1983) 1386–1392.
- [51] J.M. Manners, K.J. Scott, Reduced translatable messenger RNA activities in leaves of barley infected with *Erysiphe graminis f.sp. hordei*, *Physiol. Plant Pathol.* 26 (1985) 297–308.
- [52] T. Tani, H. Yamamoto, Nucleic acid and protein synthesis in association with the resistance of oat leaves to crown rust, *Physiol. Plant Pathol.* 12 (1978) 113–121.
- [53] H. Yamamoto, T. Tani, H. Hokin, Protein synthesis linked with resistance of oat leaves to crown rust fungus, *Ann. Phytopath. Soc. Japan* 42 (1976) 583–590.
- [54] R.A. Heinz, H. Esteban Hopp, E.A. Favret, Proteins associated with specific host–pathogen relationships in infections with wheat rust, *Plant Cell Physiol.* 31 (1990) 1221–1227.
- [55] M. Zuk, R. Weber, J. Szopa, 14-3-3 Protein down-regulates key enzyme activities of nitrate and carbohydrate metabolism in potato plants, *J. Agric. Food Chem.* 53 (2005) 3454–3460.